

Exceptional service in the national interest



Micro-structural Stress Modeling of Brittle Materials for Enhanced Performance and Reliability

M.C. Teague, S.J. Grutzik, T.E. Buchheit,, R.L. Johnson,
S.P. Meserole, and K.G. Ewsuk

Sandia National Laboratories
Albuquerque, NM 87185

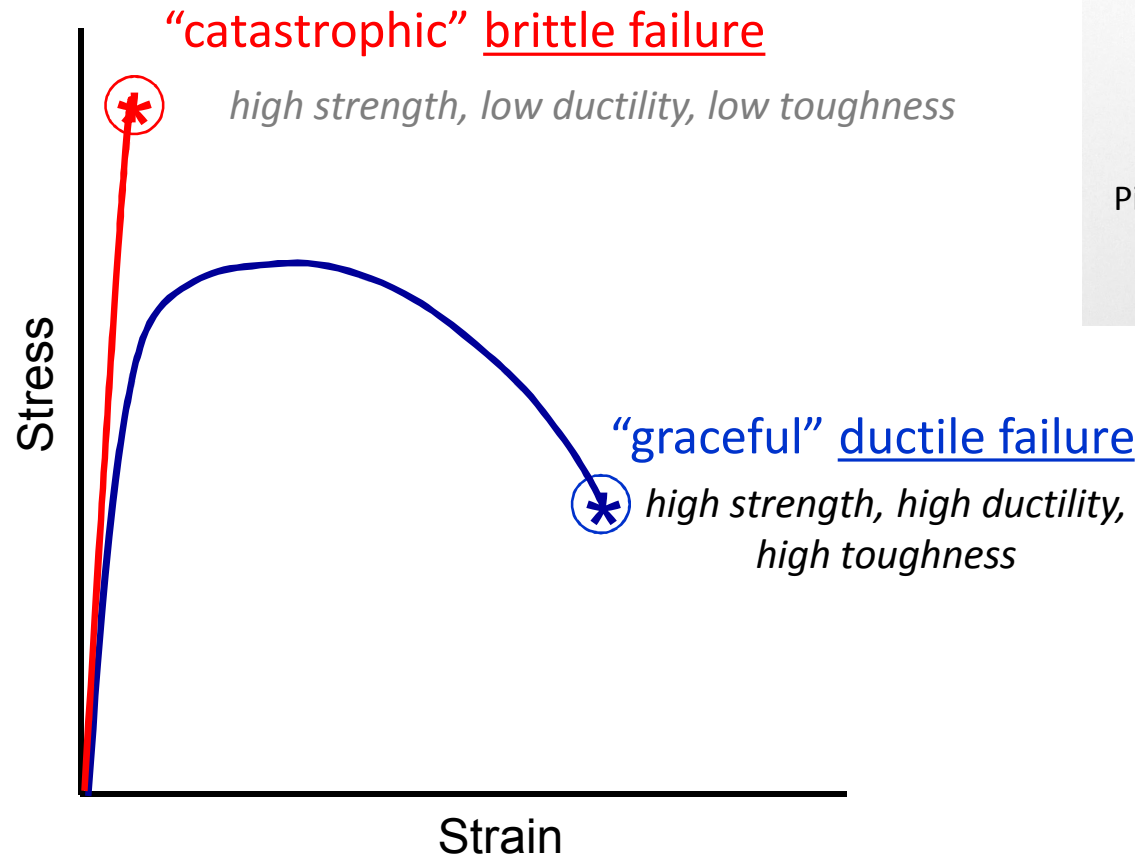
Sandia National Laboratories is a multi-program laboratory managed and operated by Sandia Corporation, a wholly owned subsidiary of Lockheed Martin Corporation, for the U.S. Department of Energy's National Nuclear Security Administration under contract DE-AC04-94AL85000.



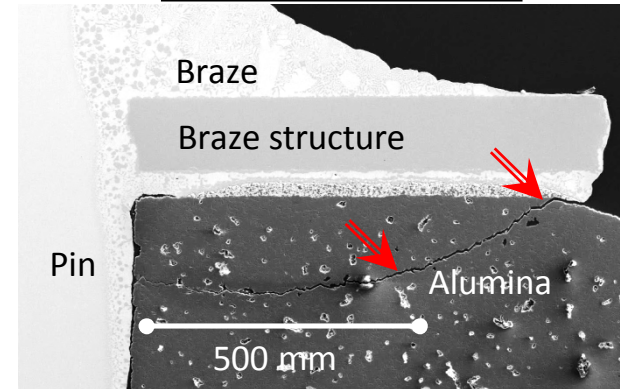
Outline

- Motivation
- Background
- Experimental Measurements
- Modeling
 - Micro-structure meshing
 - Modeling of stresses
- Future Work

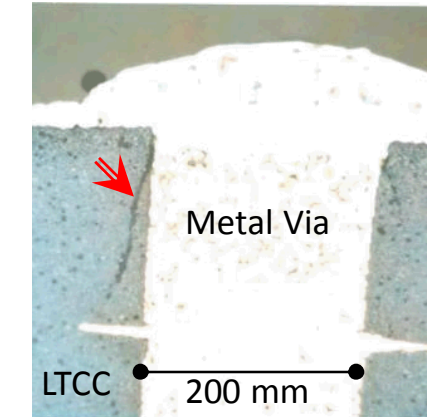
Brittle Materials Failure Presents A Reliability Concern in High Consequence Applications



Electrical Feedthru



Electronic Substrate

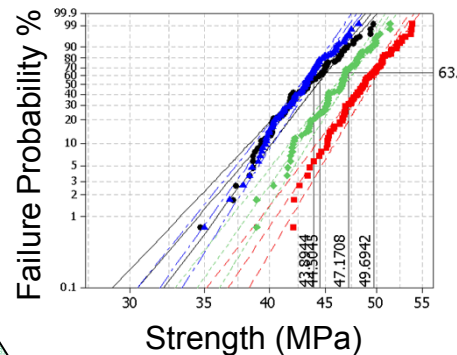
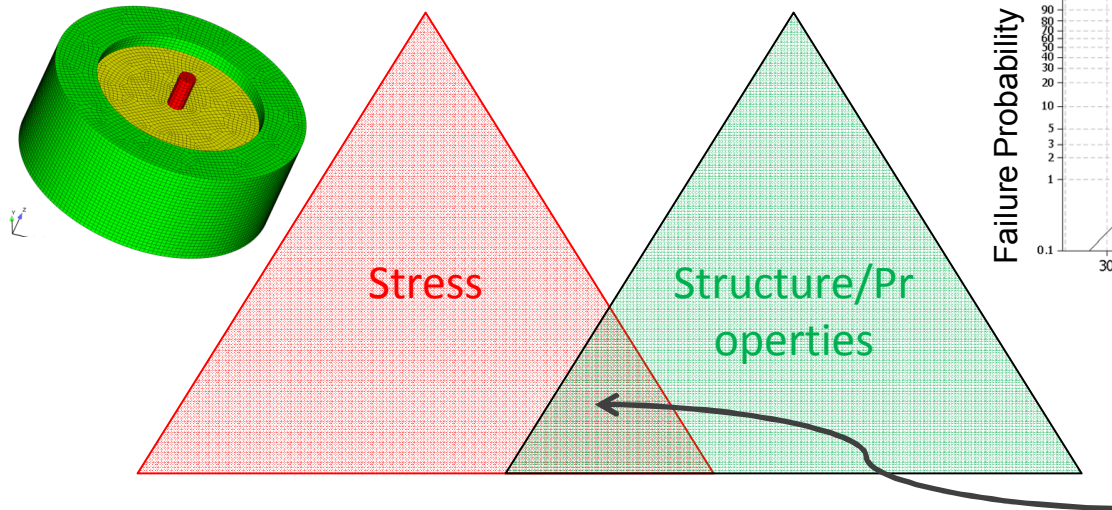


Brittle materials are susceptible to sudden catastrophic failure

Current State:

Qualitative Stress-Based Predictions

$$\sigma \sim \sigma_{crit}$$

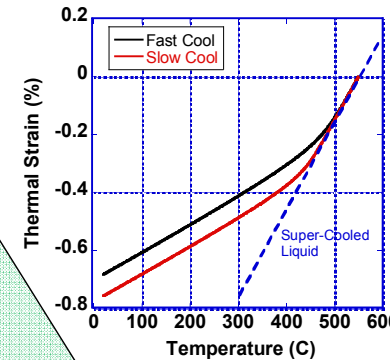
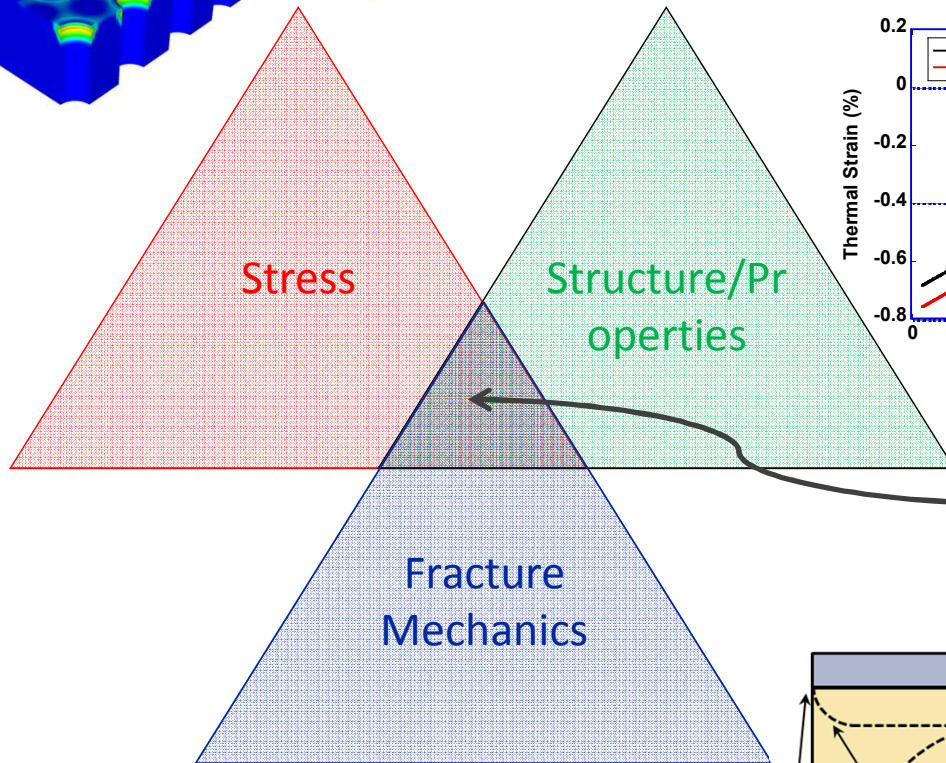
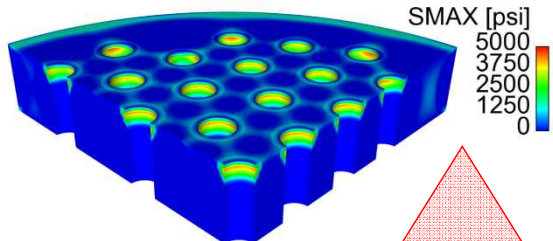


*Qualitative prediction
of brittle failure based
on engineering
judgment/experience*

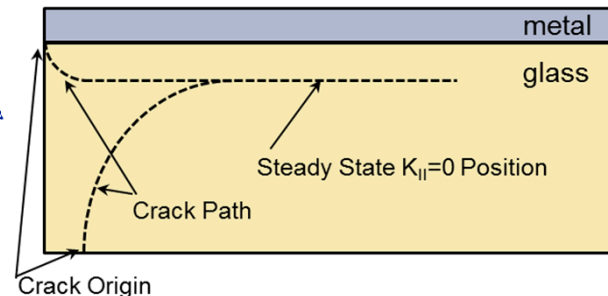
- *We Design To Avoid High Stress*
- *Engineering Judgment Has Deficiencies*
 - Limited by practical experience
 - Neglects flaws/flaw populations
 - Does not incorporate fracture mechanics

Future State: Quantitative Mechanics-Based Prediction of Brittle Failure & Reliability

$$K \sim \sigma a^{1/2} \sim K_{IC}$$



Quantitative mechanics-based brittle failure prediction



Sandia Has A Research & Development Program That Addresses The Gaps To Predict Brittle Failure



Vision

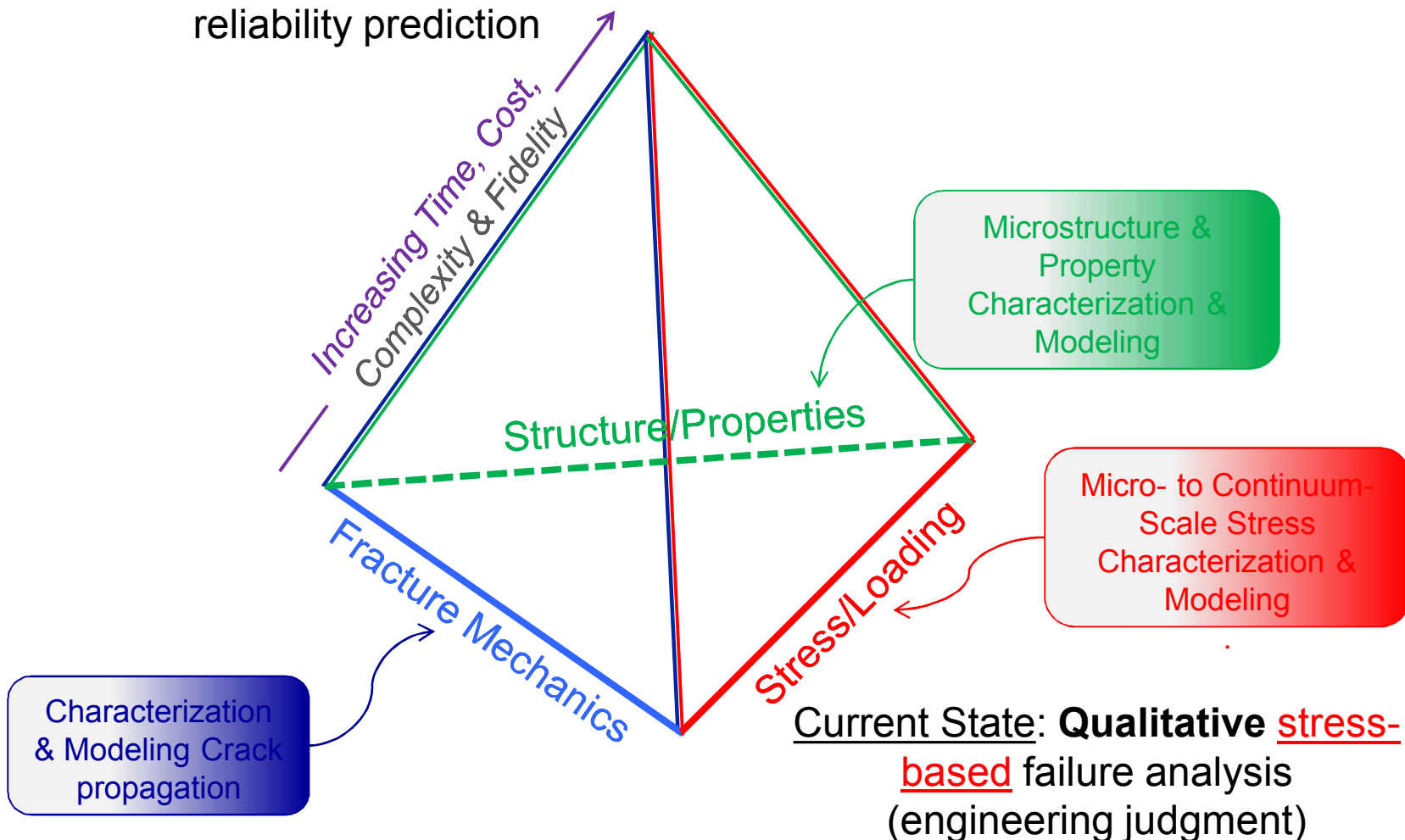
- Transition from **Qualitative** stress-based engineering judgment to **Quantitative** mechanics-based failure prediction.

Approach

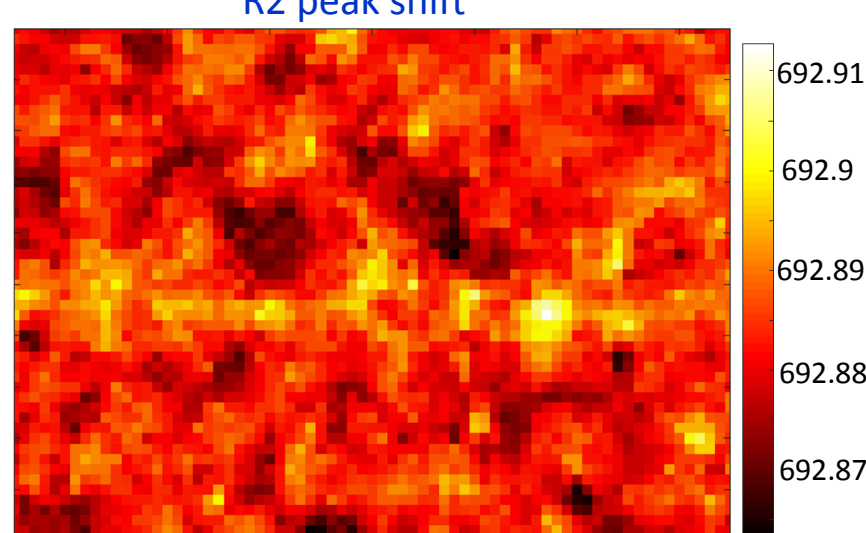
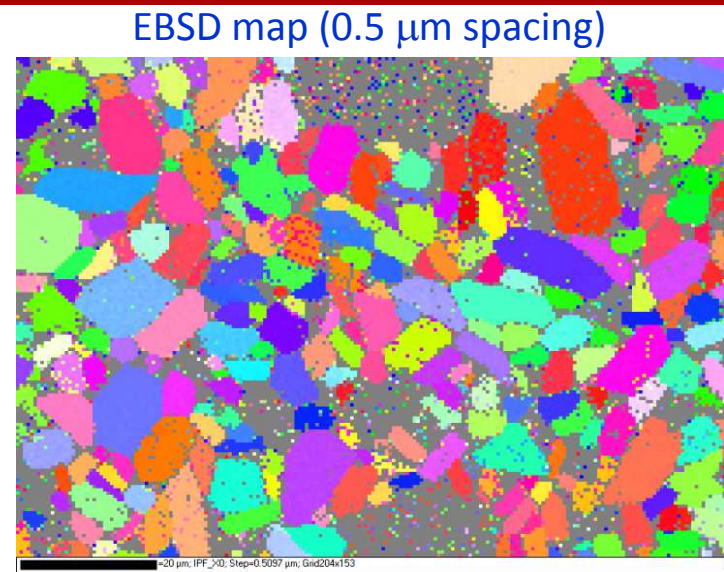
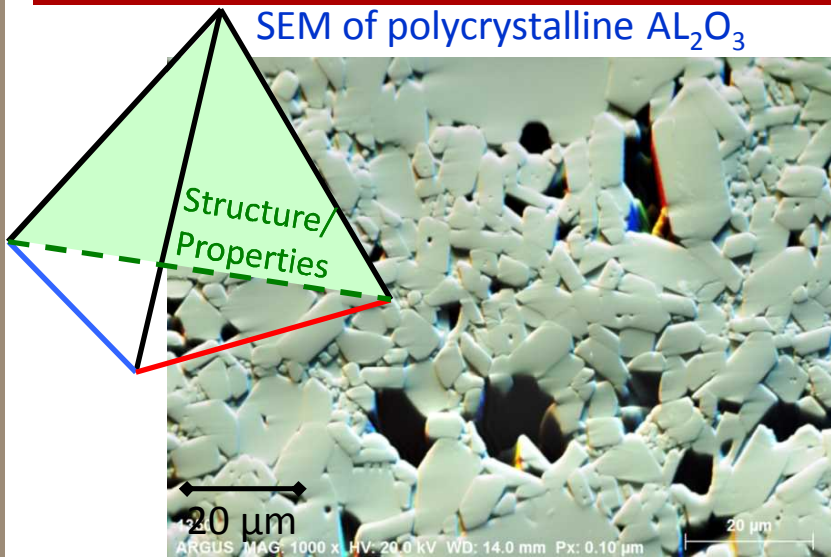
- Develop foundational materials characterization & modeling S&T in:
 - 1) **Stress/Loading** – physically-based models, materials & processing data, & model validation
 - 2) **Fracture Mechanics** - crack initiation & propagation, and statistical bounds & variability
 - 3) **Structure/Properties** – understand & control of process-structure-property relations

Coordinated Stress, Fracture, & Structure/Props Experiments & Modeling Are Being Conducted

Vision: Quantitative mechanics-based failure & reliability prediction



Micro- To Continuum-Scale Stress Mapping Is Possible With SEM/EBSD And PL Spectroscopy



PL Spectroscopy Was Used To Measure Stress-Sensitive Cr Emission Band Peak Shifts

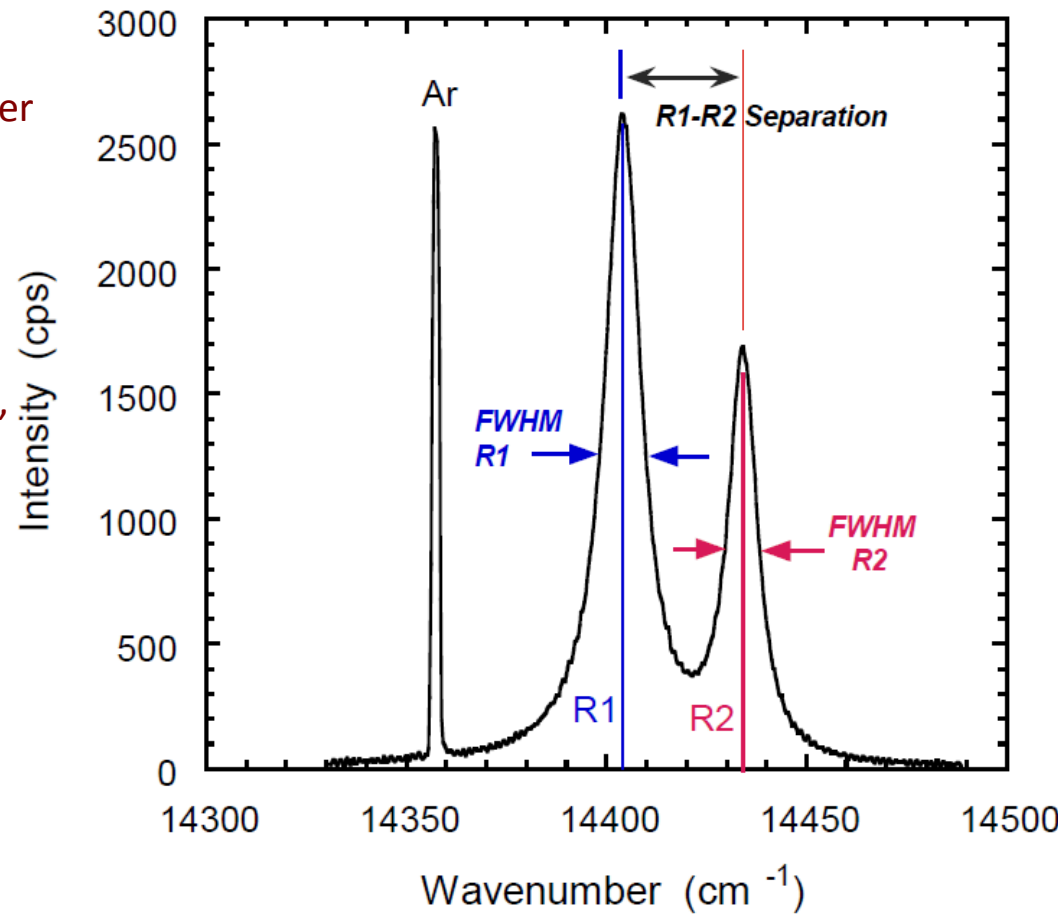
Photoluminescence (PL) Spectroscopy

Equipment

- Horiba Labram HR Raman Spectrometer
- 532 nm, 15 mW Laser
- Confocal microscope

Measurement

- Peaks shift due to stress, temperature, & Cr concentration
- Crystal orientation dependent signal
- R1 – R2 separation variation provides additional stress-state information
- Peak width provides stress-state information
- Ar line corrected instrument drift



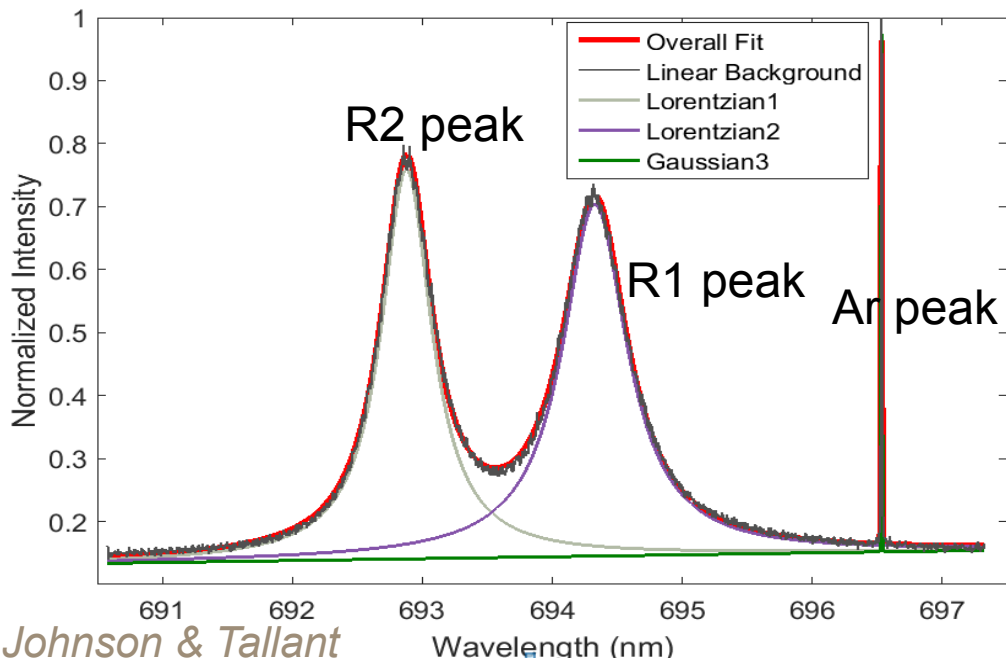
A State-Of-The-Art PL Spectroscopy Capability Has Been Developed To Map Multi-Scale Stress

Map mm^2 areas using thousands of spectra with micrometer-scale spatial resolution

- Focused laser beam for micro-scale spatial resolution
- Determine stress sensitive R1 (~ 694.24 nm) and R2 (~ 692.84 nm) Ruby ($\text{Al}_2\text{O}_3:\text{Cr}^{3+}$) PL bands
- Automated specimen repositioning and spectra acquisition
- Process thousands of spectra in minutes (MATLAB, GRAMS, & LABSPEC)

Wavelength resolution and stability to resolve peak shifts to 0.001 nm (~ 3 MPa)

- Instrument drift corrected to Ar lamp emission line NIST reference (696.5431 nm)
- Temperature stable to 0.1°C (0.0007 nm peak shift) and temperature corrected
- Working to correct for Cr concentration (1 wt.% Cr – 4.8 nm peak shift)



- R1 & R2 fluorescence peaks (positions, widths, and separations) are best fit with a Lorentzian or pseudo-Voigt fit
- The Ar peak is best fit with a Gaussian fit

Converting Peak Shifts to Stress

$$\Delta\nu \text{ (1/cm)} = \Pi_{ij} \left(\frac{\text{cm}^{-1}}{\text{GPa}} \right) \sigma_{ij} \text{ (GPa)}$$

if $\Pi_{11} = \Pi_{22} = \Pi_a$ and $\Pi_{33} = \Pi_c$ this can be put in the form

$$\begin{bmatrix} \Delta\nu^{(1)} \\ \Delta\nu^{(2)} \end{bmatrix} = \begin{bmatrix} \Pi_M^{(1)} & \Pi_S^{(1)} \\ \Pi_M^{(2)} & \Pi_S^{(2)} \end{bmatrix} \begin{bmatrix} \sigma_M \\ \sigma_S \end{bmatrix} \text{ where } \begin{aligned} \Pi_M^{(i)} &= \Pi_c^{(i)} + 2\Pi_a^{(i)} & \Pi_S^{(i)} &= \Pi_c^{(i)} - \Pi_a^{(i)} \\ \sigma_M &= (\sigma_{11} + \sigma_{22} + \sigma_{33})/3 & \sigma_S &= (2\sigma_{33} - \sigma_{11} - \sigma_{22})/3 \end{aligned}$$

C. A. Michaels, R. F. Cook, "Determination of residual stress distributions in polycrystalline alumina using fluorescence microscopy" *Materials and Design*, 107, (2016), 478-490

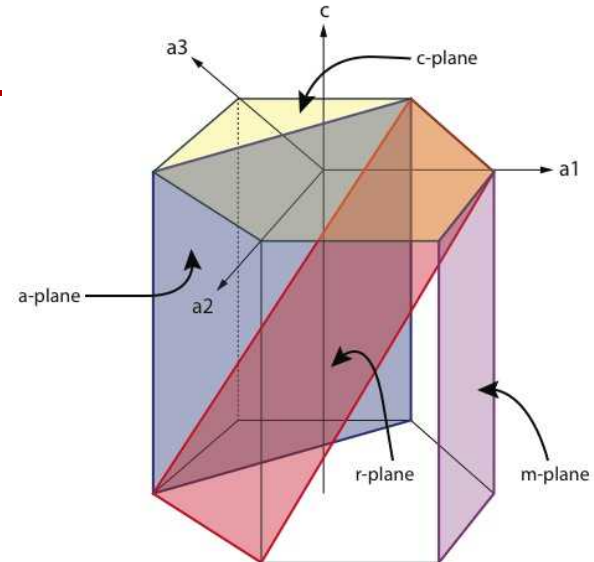
Table I. Piezospectroscopic Coefficients for Ruby

		Piezospectroscopic coefficients (cm ⁻¹ /GPa)						
		Previous results		Our results				
		Uniaxial loading		Hydrostatic loading pressure coeff P^{\dagger}	Π_{11}	Π_{22}	Π_{33}	$\Pi_{11} + \Pi_{22} + \Pi_{33}$
R1	Π_{11}	Π_{33}	P^{\dagger}	7.59 ^{††}	2.56	3.50	1.53	7.59
	3.0 [‡]	1.8 [‡]		7.59 ^{††}	2.56	3.50	1.53	7.59
	3.2 [§]	1.4 [§]		7.59 ^{††}	2.56	3.50	1.53	7.59
R2	2.7 [¶]	1.8 [¶]	P^{\dagger}	7.615 ^{††}	2.65	2.80	2.16	7.61
	2.8 [‡]	2.3 [‡]		7.615 ^{††}	2.65	2.80	2.16	7.61
	2.8 [§]	1.9 [§]		7.615 ^{††}	2.65	2.80	2.16	7.61
	2.4 [¶]	2.2 [¶]		7.615 ^{††}	2.65	2.80	2.16	7.61

[†] $P = \Pi_{11} + \Pi_{22} + \Pi_{33}$ [‡]Reference 4, room temperature(?). [§]Reference 7, 77 K. [¶]Reference 6, 77 K. ^{††}Reference 12, room temperature.

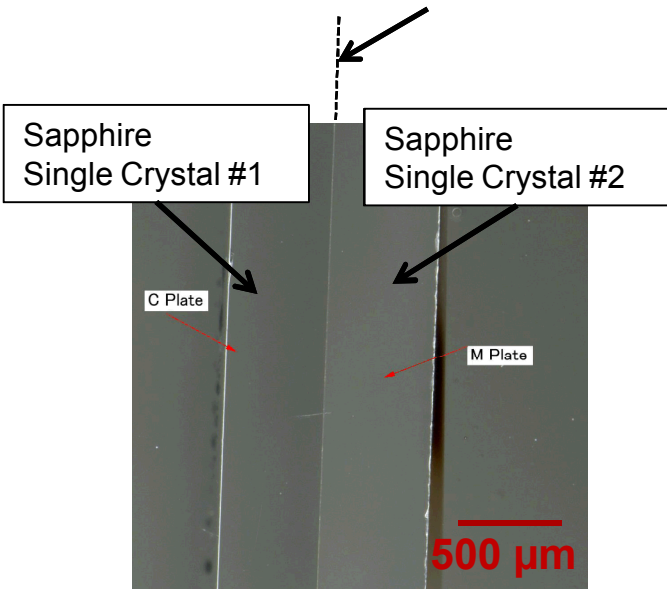
Bi-crystal samples for Spectroscopic stress measurement

- Sputtered ~100nm of glass on polished surface of single crystals (Eagle glass from corning)
- Crystals were then placed glass side together on alumina boat
- Crystals were heated to 1600°C at 20°C/min and held for 1 hr followed by air cool in furnace



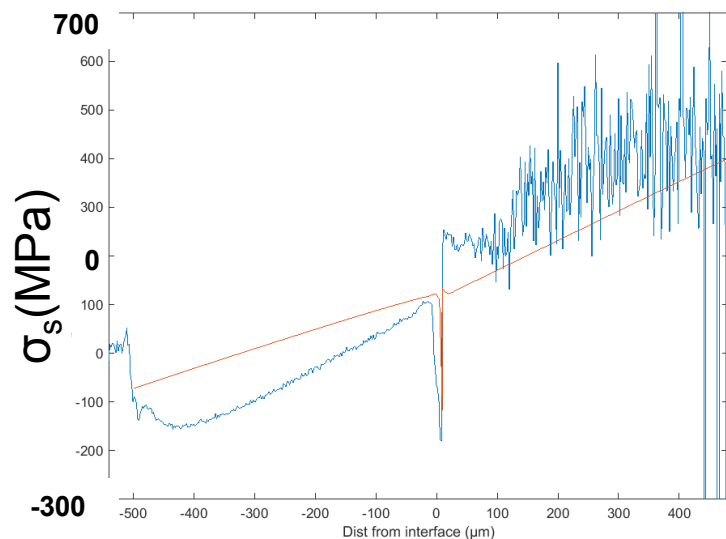
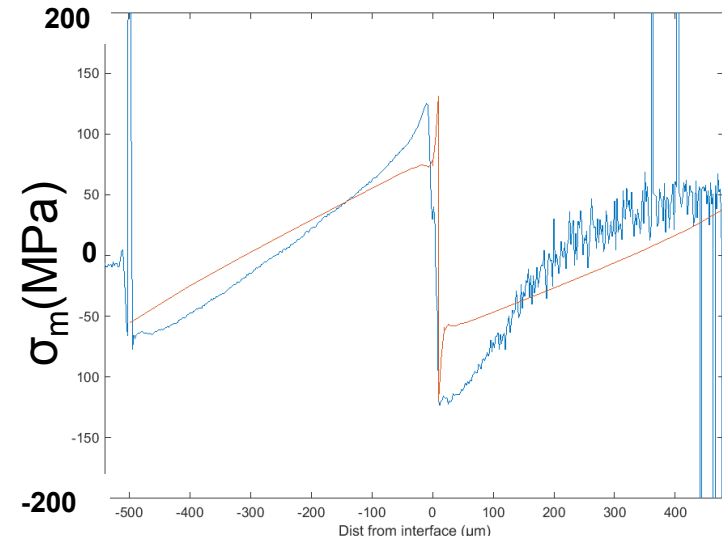
Successfully bonded Bi-crystals:

- C-plane to C-plane, rotated 30°
- A-plane to C-plane
- A-plane to M-plane



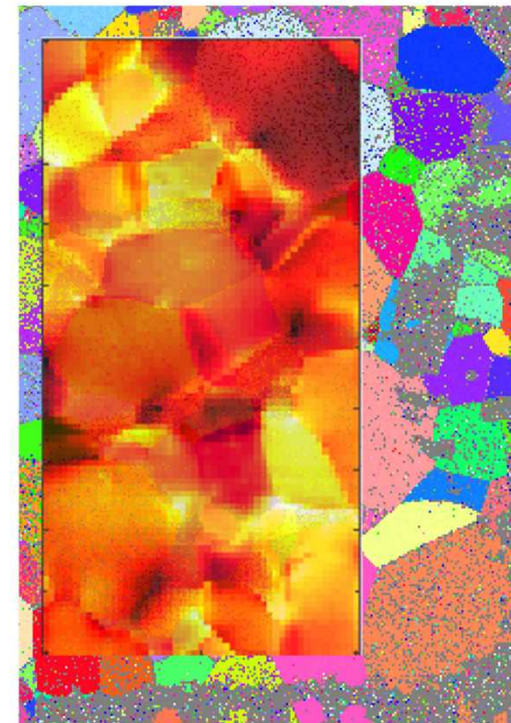
Stress results, compare to FE

- σ_M calculated from PL data has same shape as that from FE model
- There is currently a scaling uncertainty
 - What temperature change should be applied in FE model?
 - This plot uses $\Delta T = 1600$ °C but glass layer doesn't support stress for high temperatures
 - Currently only using linear, room temperature CTE values



Microstructural Meshing REAL microstructures

- Generated microstructures are often insufficient for model validation with experiments
- Equivalent microstructures is vaguely defined, in order to do first order model validation need microstructure upon which experiments performed

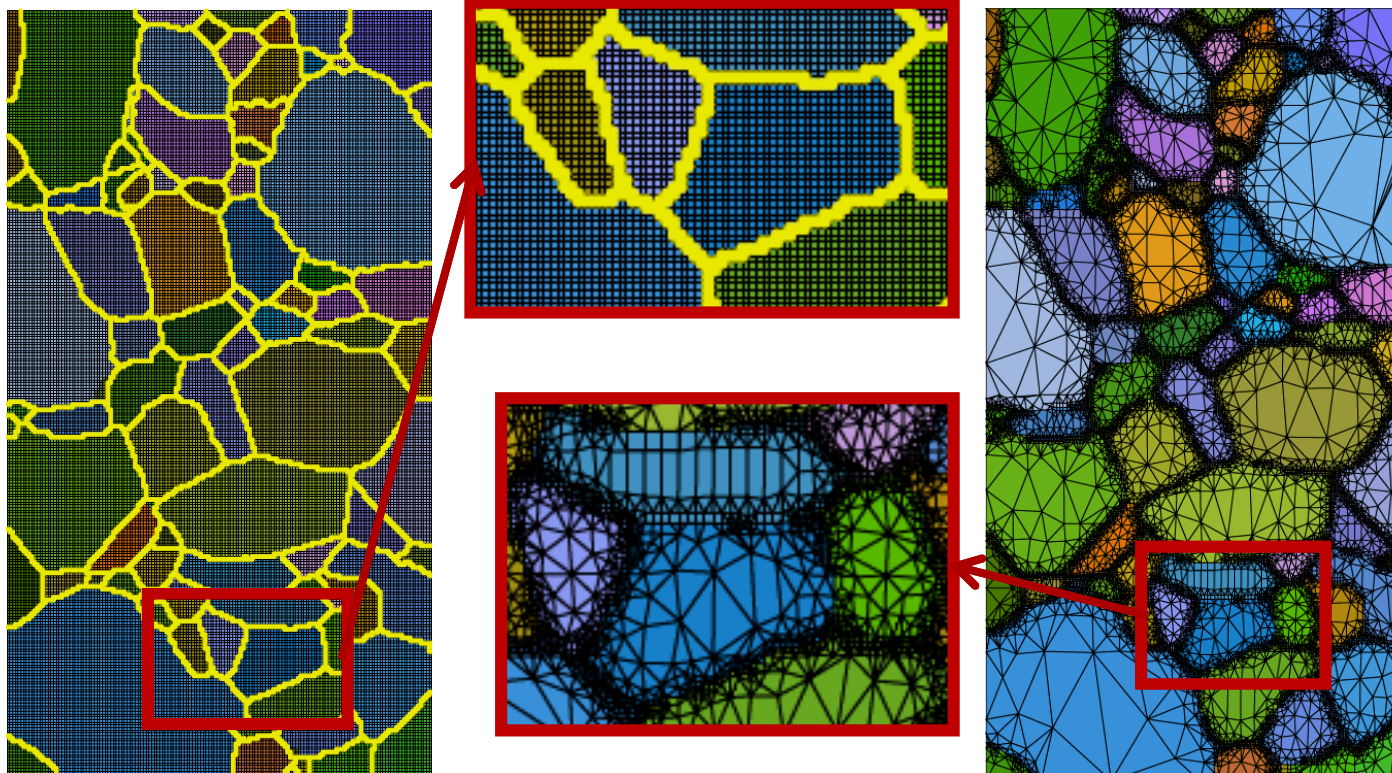


EBSD map aligned with experiment mapped for stress

Meshing Schemes

- Multiple commercial and open source meshing software's available
- Common issue is number of elements to capture microstructure can become extremely large
- Fall into two basic categories
 - Point-by-point, or element for every pixel/data point
 - Cubit Sculpt, MOOSE EBSD/Image reader, etc
 - Software that enables input from multiple data sources
 - OOF2/3D, Avizo, etc

Comparisons of Meshing Schemes

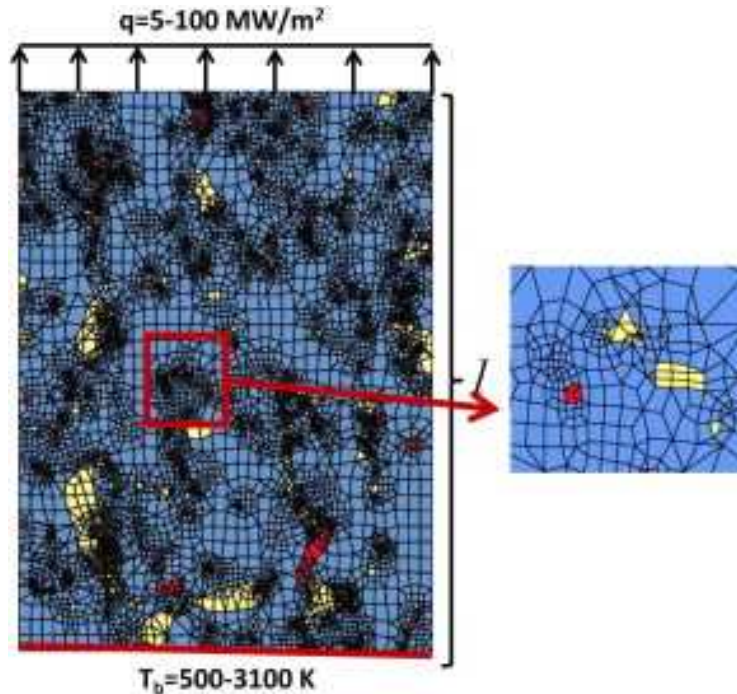


	Element per point	OOF2
$N_{elements}$	44274	18090
N_{nodes}	43836	27987

Significant reduction in computational power for OOF2 meshes

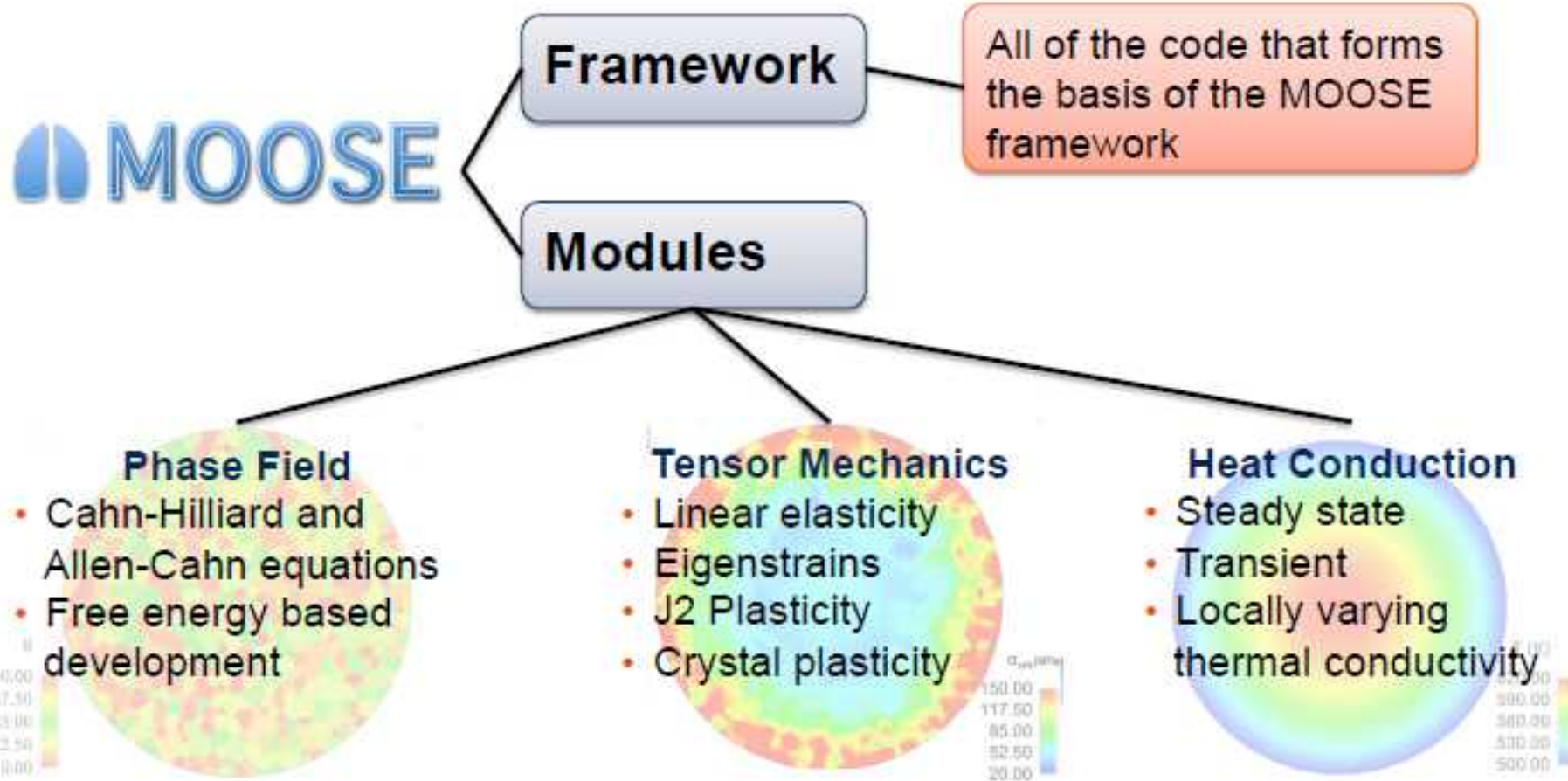
Have your mesh now what?

- Need material properties, including anisotropy
- Need to be able to rotate elasticity and other tensor properties by orientation
- MOOSE is great option for adaptive rapid development



Mesoscale Modeling with the MOOSE framework

- All of the code required to easily create your own phase field application is in the open source MOOSE modules (MOOSE-PF).



Model Set up

elastic constants

$$S_{11} = 497 \text{ GPa} \quad S_{33} = 501 \text{ GPa}$$

$$S_{44} = 147 \text{ GPa} \quad S_{12} = 163 \text{ GPa}$$

$$S_{13} = 116 \text{ GPa} \quad S_{14} = -22 \text{ GPa}$$

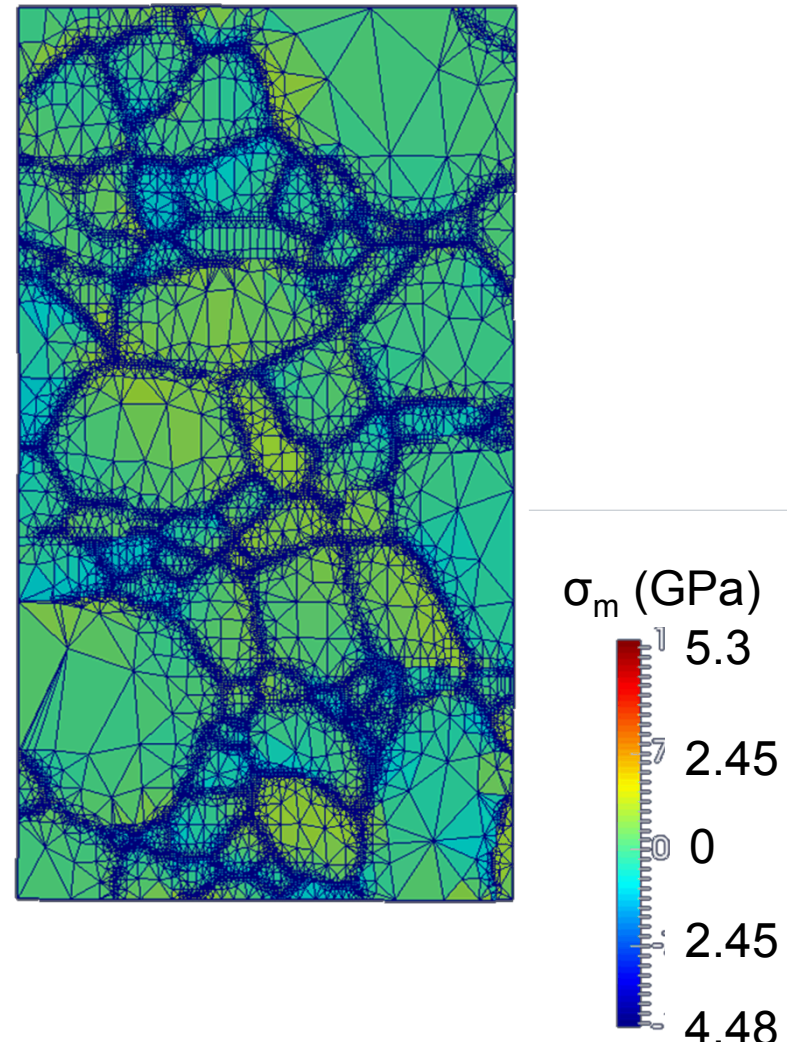
- Goto et. al. Journal of Geophysical Research, 1989

Coefficients of thermal expansion

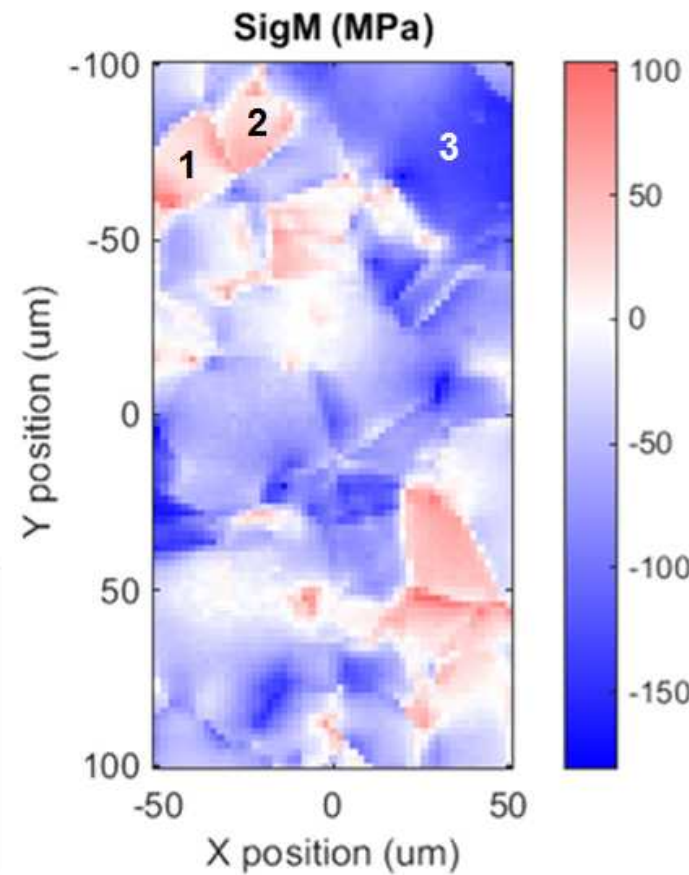
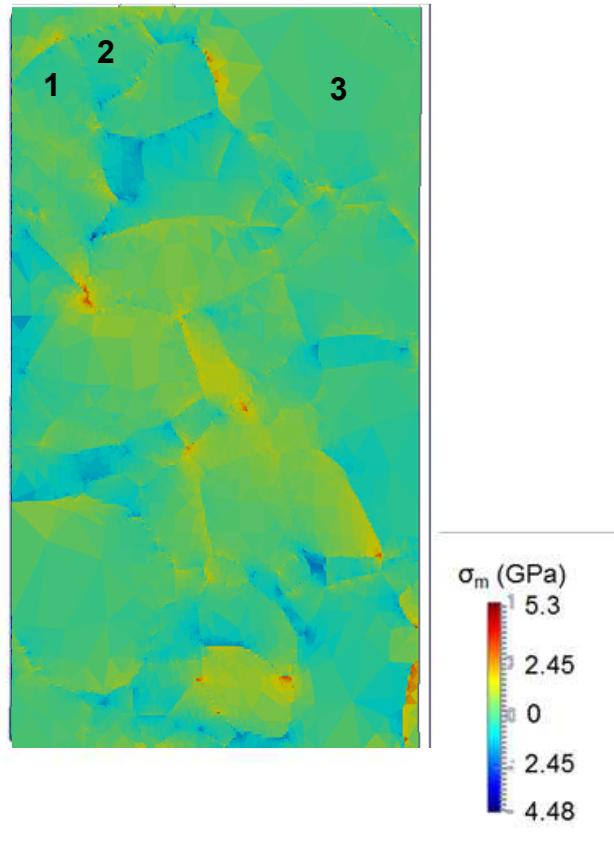
$$\alpha_{11} = 7.3 \times 10^{-6} \text{ 1/}^{\circ}\text{C}$$

$$\alpha_{33} = 8.2 \times 10^{-6} \text{ 1/}^{\circ}\text{C}$$

$$\Delta T = 1500^{\circ}\text{C}$$



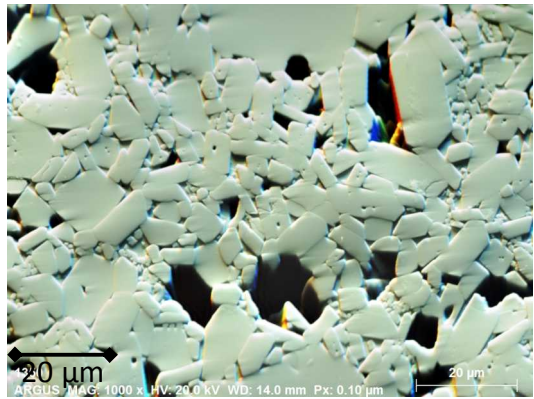
Comparison to Experiment



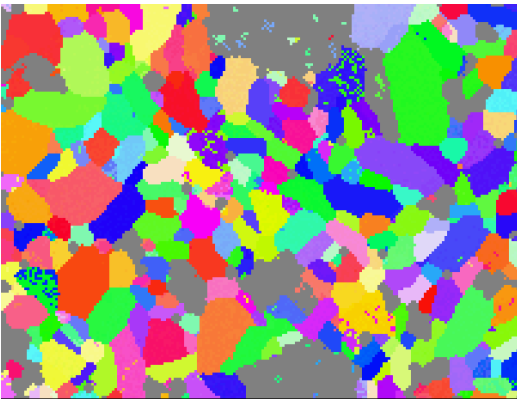
General Agreement-need to refine
for resolution and 2D-3D reality

Grain	σ_m (MPa)
1	49
2	206
3	-52

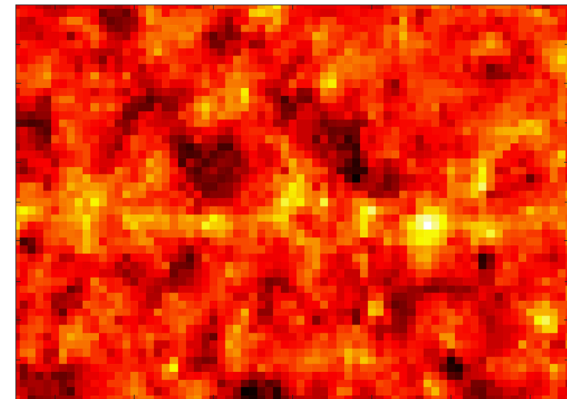
Experimentally-Informed Microstructure Modeling Capability Is Being Developed To Predict Stress



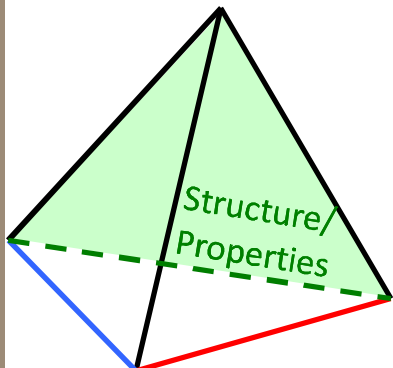
SEM of Al_2O_3



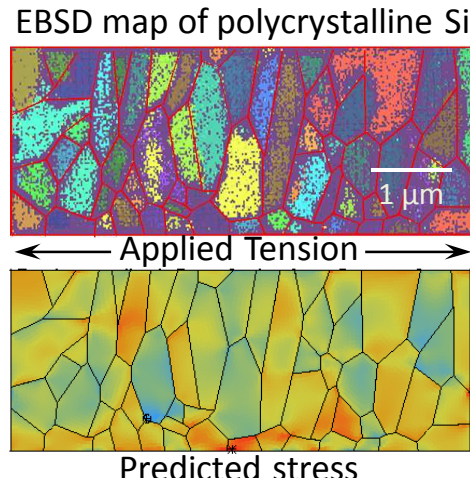
EBSD map of Al_2O_3



Stress map of Al_2O_3

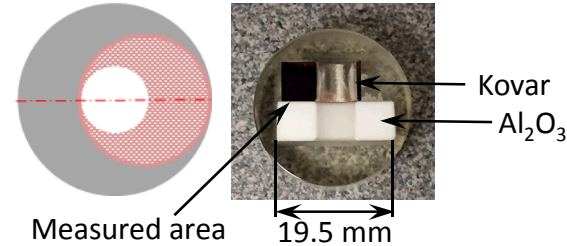


1.29 (GPa) 1.96
Von-Mises Stress

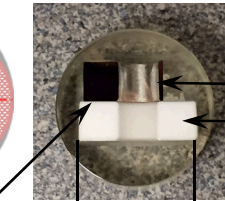


FE simulation of micro-scale stress & variation in a brittle material microstructure

Al_2O_3 – Kovar Brazed Sample

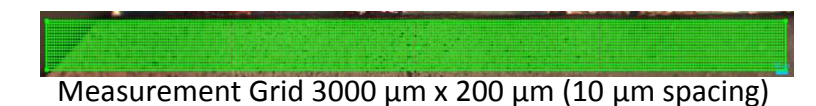


Measured area

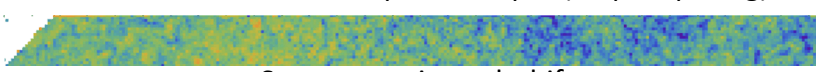


Kovar

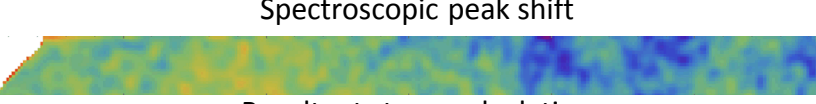
Al₂O₃



Measurement Grid 3000 μm x 200 μm (10 μm spacing)



Spectroscopic peak shift



Resultant stress calculation

-100 0 100 (MPa)

PL spectroscopy used for micro- to continuum-scale stress measurement

Conclusions

- Photo-luminescence spectroscopy mapping is promising technique for enabling validation of stress at critical microstructural level
- Ease/speed of experiments enables large areas to be measured
- Microstructure meshing and modeling are primed to take advantage of this new data to enable mechanistic based models of brittle failure

Future Work

- Perform external loading experiments on single crystals
- Perform loading experiments on tested microstructures and compare
- Move to more complicated microstructures
- Study interaction of loading and microstructure defects/properties
- Improve models with experimental validation

Questions



Backup Slides



Converting Peak Shifts to Stress

$$\Delta\nu \text{ (1/cm)} = \Pi_{ij} \left(\frac{\text{cm}^{-1}}{\text{GPa}} \right) \sigma_{ij} \text{ (GPa)}$$

if $\Pi_{11} = \Pi_{22} = \Pi_a$ and $\Pi_{33} = \Pi_c$ this can be put in the form

$$\begin{bmatrix} \Delta\nu^{(1)} \\ \Delta\nu^{(2)} \end{bmatrix} = \begin{bmatrix} \Pi_M^{(1)} & \Pi_S^{(1)} \\ \Pi_M^{(2)} & \Pi_S^{(2)} \end{bmatrix} \begin{bmatrix} \sigma_M \\ \sigma_S \end{bmatrix} \text{ where } \begin{aligned} \Pi_M^{(i)} &= \Pi_c^{(i)} + 2\Pi_a^{(i)} & \Pi_S^{(i)} &= \Pi_c^{(i)} - \Pi_a^{(i)} \\ \sigma_M &= (\sigma_{11} + \sigma_{22} + \sigma_{33})/3 & \sigma_S &= (2\sigma_{33} - \sigma_{11} - \sigma_{22})/3 \end{aligned}$$

C. A. Michaels, R. F. Cook, "Determination of residual stress distributions in polycrystalline alumina using fluorescence microscopy" *Materials and Design*, 107, (2016), 478-490

Table I. Piezospectroscopic Coefficients for Ruby

	Piezospectroscopic coefficients (cm ⁻¹ /GPa)						
	Previous results			Hydrostatic loading pressure coeff P^*	Our results		
	Uniaxial loading				Π_{11}	Π_{22}	Π_{33}
R1	Π_{11}	Π_{33}		7.59 ^{††}	2.56	3.50	1.53
	3.0 [‡]	1.8 [‡]					7.59
	3.2 [§]	1.4 [§]					
R2	2.7 [¶]	1.8 [¶]					
	2.8 [‡]	2.3 [‡]		7.615 ^{††}	2.65	2.80	2.16
	2.8 [§]	1.9 [§]					
	2.4 [¶]	2.2 [¶]					7.61

[†] $P = \Pi_{11} + \Pi_{22} + \Pi_{33}$ [‡]Reference 4, room temperature([?]). [§]Reference 7, 77 K. [¶]Reference 6, 77 K. ^{††}Reference 12, room temperature.